ELSEVIER

Enhanced performance of the OLED with plasma treated ITO and plasma polymerized thiophene buffer layer

Sang-Moo Park [a,*], Kenji Ebihara [a], Tomoaki Ikegami [a], Boong-Joo Lee [b], Kyung-Bum Lim [c], Paik-Kyun Shin [d]

[a] Graduate School of Science and Technology and Department of Electrical and Computer Engineering, Kumamoto University, 2-39-1 Kurokami, Kumamoto 860-8555, Japan
[b] Digital Display Research Laboratory, LG Electronics, 16 Woomyeon-Dong, Seocho-Gu, Seoul 137-724, Republic of Korea
[c] Korea Fire Safety Association, 87-4, 8-Ga, Youngdeungpo-Dong, Youngdeungpo-Gu, Seoul 150-038, Republic of Korea
[d] School of Electrical Engineering, Inha University, 253 Yonghyun-Dong, Nam-Gu, Incheon 402-751, Republic of Korea

Abstract

In this work, indium-tin-oxide (ITO) electrode in organic light emitting device (OLED) was modified by using an O_2 plasma treatment and plasma polymerized thiophene buffer layers were inserted between ITO (anode) and organic layer in order to improve the hole injection efficiency. Furthermore, electron injection to cathode (Al) in the test OLED seemed to be improved due to introduction of quantum well in the cathode. The plasma-polymerized thiophene buffer layer on the O_2 plasma-treated transparent ITO electrode seemed to result in formation of a stable interface and consequently, reduction the hole mobility, which in turn caused enhanced recombination of hole and electron in the emitting layer. Compared with the test device without buffer layer, the turn-on voltage of the test device with the buffer layer was lowered by 1.0 V.
© 2006 Elsevier B.V. All rights reserved.

1. Introduction

Organic light-emitting devices (OLEDs) based on organic layers have been extensively studied for potential applications, especially in the field of flat-panel displays [1–4]. Anodes of OLEDs commonly comprised a transparent conducting oxide (TCO). Indium tin oxide (ITO) has been widely used as an attractive anode material because of its high transparency, high conductivity and high work function [5–7]. However, an OLED formed on a bare ITO surface usually shows insufficient hole injection efficiency and unacceptable operation stability. The interface between the electrode and organic layer in OLEDs affects the charge injection process and consequently result in deterioration of the electrical and luminescent properties. In particular, the morphology and oxygen defects on the ITO surface are known to be important factors for the charge injection efficiency at the interface. Hung et al. [8] managed to deposit a CHF_3 buffer layer on ITO at low frequency. The devices showed superior operation stability, but the influence of the CHF_3 buffer layer on the device efficiency was not reported. In this work, we deposited a plasma polymerized thiophene (ppTh) thin film at radio frequency on ITO, and the effect of ppTh on the device efficiency and stability was investigated. Furthermore, we investigated about the surface treatment of ITO electrode and the growth method of a new buffer layer by using RF plasma-polymerization equipment to improve the efficiency of OLEDs.

* Corresponding author. Fax: +81 96 342 3630.
E-mail address: smpark@st.eecs.kumamoto-u.ac.jp (S.-M. Park).

2. Experimental details

2.1. Fabrication of test devices

The substrates used in this study were ITO coated glasses with ITO film thickness of 2000 Å and sheet resistance of 23 Ω/sq. The as-received substrates were ultrasonically cleaned in deionized water, acetone and methanol, by which most of the surface organic contaminants were removed. After nitrogen blow-drying, the cleaned ITO substrate was then moved into a vacuum chamber. Capacitive-coupled plasma polymerization equipment was used for RF plasma surface treatment of the ITO. A schematic diagram of the plasma-polymerization apparatus used in this experiment is shown in Fig. 1 [9]. A 13.56-MHz RF plasma generator (AUTO ELEC. ST-500) with a matching box was connected to the electrodes. The ppTh was polymerized at the following experimental conditions: 100 W power, 0.1 torr system pressure. A commercial thiophene monomer was used to deposit the ppTh thin film as a buffer layer: Ar gas was introduced into the reaction tube at a flow rate of 10 sccm to generate the RF plasma, and then the thiophene monomer was introduced into the reactor.

In this research, N,N-diphenyl-N,N-(3-methyphenyl)-1,1-biphenyl-4-4-diamine (TPD), known as a hole transporting material and tris (8-hydroxyquinolinato)-aluminum (Alq$_3$), which is an electron-transporting material were deposited at a base pressure of 5×10^{-5} torr. Deposition rates of the TPD and Alq$_3$ were 2 Å/s, respectively, which were measured by using a thickness monitor. Then a 1500 Å thick Al cathode was deposited at the same pressure.
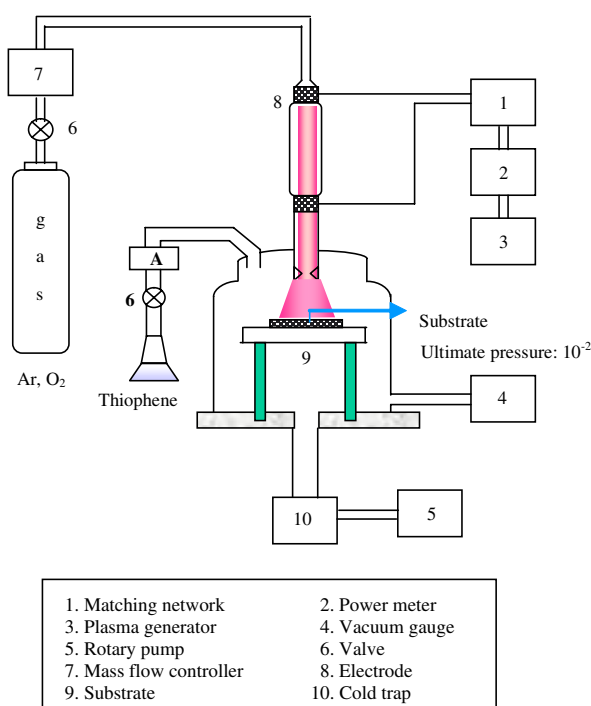

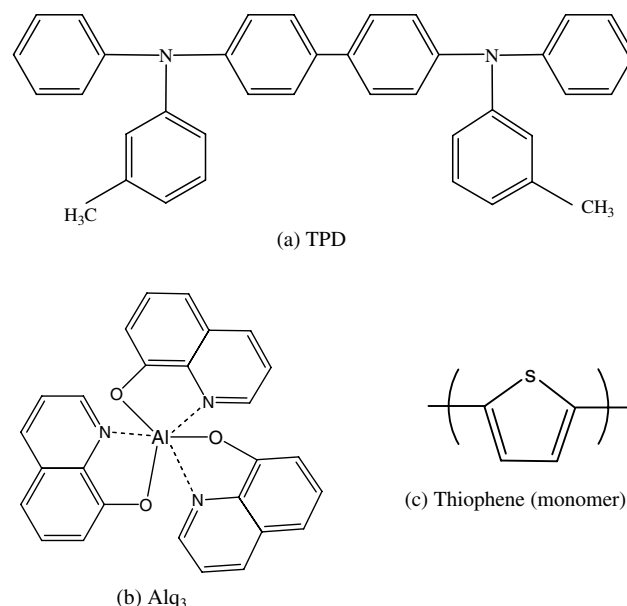Fig. 1. Schematic diagram of the plasma polymerization apparatus.

1. Matching network
2. Power meter
3. Plasma generator
4. Vacuum gauge
5. Rotary pump
6. Valve
7. Mass flow controller
8. Electrode
9. Substrate
10. Cold trap

(a) TPD

(b) Alq$_3$

(c) Thiophene (monomer)

Fig. 2. Molecular structures of the organic materials.

The area of each electrode was 2×2 mm^2. Fig. 2 shows the molecular structures of the organic materials.

2.2. Current–voltage–luminance measurement

Current and luminance characteristics of the test OLED devices according to applied voltage change were measured by a source measurement unit (SMU; Keithley, model 2400) and luminance meter (TOPCON, BM-8). A personal computer was used for an automated measurement system: the SMU controlled the supply of the source voltage through a GP-IB interface and measured the current. At the same time, the luminance meter measured luminance through a RS-232C interface. The increment of the applied voltage was 0.3 V/0.5 s.

3. Results and discussion

3.1. Material properties characterization

Since the hole transport layer (HTL) film of the device is directly deposited on the ITO anode, the surface properties of the ITO affect the characteristics of the OLEDs. A high surface roughness of the ITO would cause a structural defect (i.e. charge trapping site) at the organic/metal interface and consequently deteriorate the device characteristics. Therefore it is important to optimize the surface conditions of the ITO. We observed atomic force microscopy (AFM) images of the differently treated ITO surface. Fig. 3 shows AFM surface morphologies of the ITO surface as a function of O$_2$ plasma treatment time. Roughness is a basic parameter, which indicates the deviation of a surface with respect to a perfect plane. The RMS is defined as
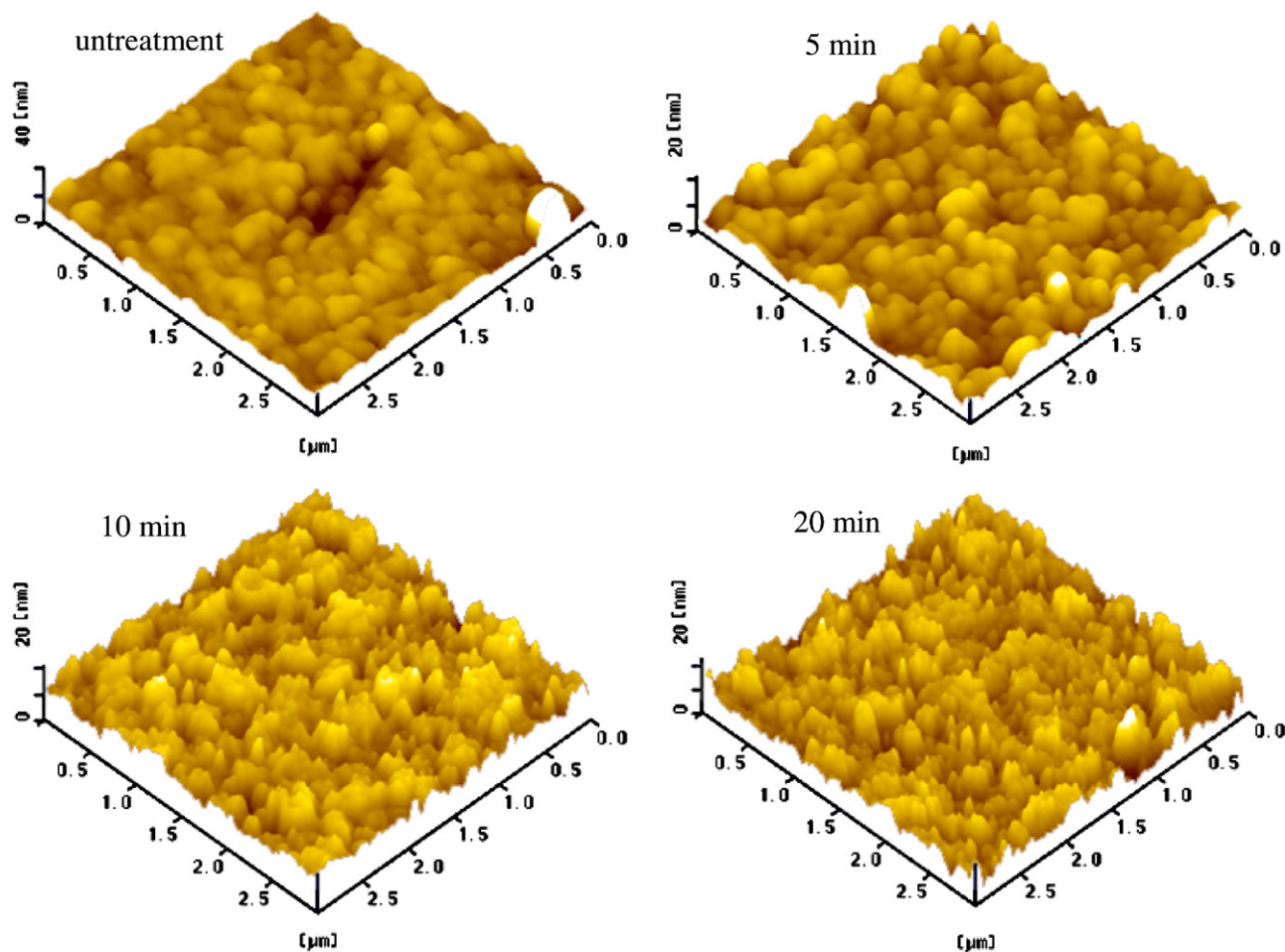
Fig. 3. AFM images of ITO surface as a function of O_2 plasma treatment time.

$$R(\text{rms}) = \sqrt{\frac{\sum_{i=1}^{N}(Z_i - Z_{\text{ave}})^2}{N}} \qquad (1)$$

where Z_i is the Z value of each point, Z_{ave} is the average of the Z values and N is the number of points. As treatment time is increased, the root mean square (RMS) decreases due to ion bombardment during the plasma process. The ITO surface roughness decreases from 21 Å to 17 Å as it is treated with O_2 plasma for 5 min. In addition, the surface roughness is changed from 17 Å to 15 Å by increasing treatment time to 20 min. As a result, it is shown that the RMS roughness of the ITO surface tends to decrease with increasing treatment time. This result implies that free radical is increased on the substrate surface when plasma treatment is done and that surface roughness is low due to electrostatic behavior when electrons collide against the surface [10,11]. This way imply that O_2 plasma treatment affects the improvement of ITO surface condition in a good way.

After the measurement of RMS of the ITO surface by AFM, X-ray photoelectron spectroscopy (XPS) was applied to identify the change of chemical structure of the ITO surface caused by O_2 plasma treatment. The XPS spectrum showed peaks at 531.0, 284.5, 459.3 and 504.0 eV from the photo-ionization of oxygen 1s (O1s), carbon 1s (C1s), indium 1s (In1s) and tin 1s (Sn1s), respectively.

In Figs. 4 and 5 [X]/[In] ratios (X = C, O, Sn) are plotted as a function of O_2 plasma treatment time. Since the [C]/[In] ratio drastically decreased after a short time of treatment, carbon contaminants were found to be easily removed by the plasma treatment. The untreated ITO showed a relatively high [O]/[In] ratio, due to surface contamination. Therefore, the decrease of the [O]/[In] ratio by the plasma treatment for 5 min is ascribed to the elimination of the contamination. On the other hand, the ITO treated for a longer time was led into surface oxidation by the oxygen containing plasma exposure. The [Sn]/[In] ratio was not changed by the plasma treatment. This means that the plasma treatment used here did not etch the ITO surface. In addition, no morphological change was confirmed by scanning electron microscopy.

As is shown in Fig. 6, the Fourier transform infrared spectroscopy (FT-IR) transmission spectrum for the ppTh contains bands that represent carbon–carbon and carbon–sulfur bonds, as well as the prominent bands that can represent carbon–oxygen, sulfur–oxygen, and carbon–nitrogen bonds. Bands (a) 3417 cm^{-1} represent hydroxyl
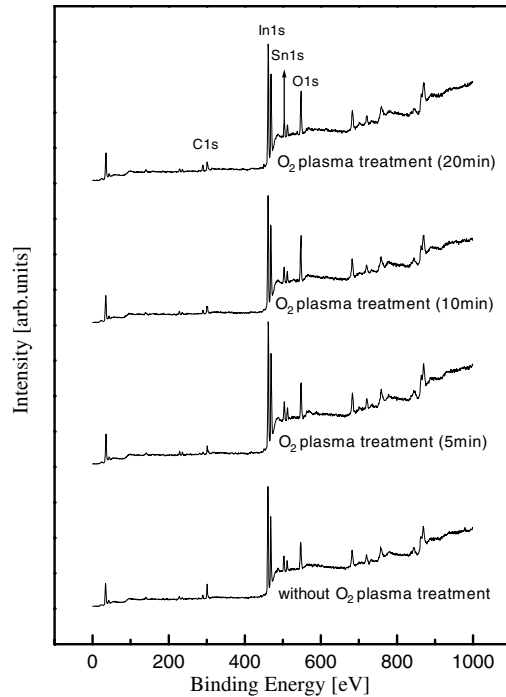
Fig. 4. ITO peaks by XPS as a function of O_2 plasma treatment time: XPS was applied to identify the change of chemical structure caused by O_2 plasma treatment.
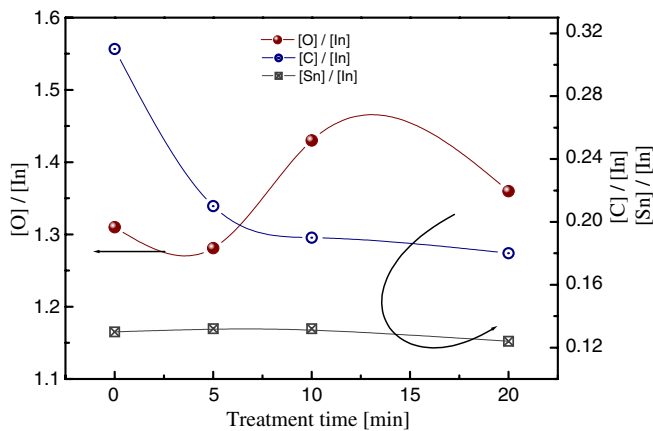

Fig. 5. Rate of [X]/[In] by XPS as a function of O_2 plasma treatment time (X = C, O, Sn). The vertical axes represent the ratio of each element to indium in the composition.

groups; bands (b) and (c) 2957 and 2861 cm^{-1} represent CH_3 and CH_2 groups; bands (d) 1674 cm^{-1} represent X–C=O, carbonyl, carboxyl; band (e) 1447 cm^{-1} represents CH_2–S [12]. The analyzed FT-IR data shown in Fig. 6 reveal that the thiophene monomer was polymerized. The sizes of [O] and [N] are shown to be large noticeably in the FT-IR spectrum of ppTh. The peak showing the thiophene ring's character is shown between 1000 and 1100 cm^{-1}, whereas this is not the case in ppTh. This result seemed to be caused either by destruction of some monomer by irradiation of the plasma's strong energy or by for-
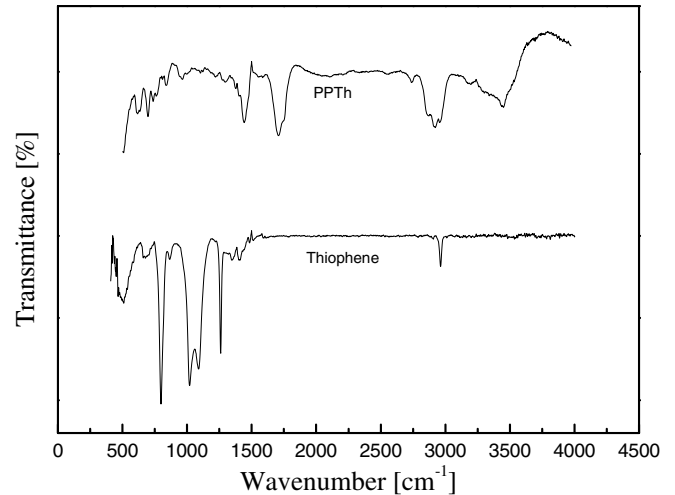

Fig. 6. FT-IR spectra of thiophene and ppTh.

mation of a new polymerization by joining with other atoms.

3.2. Electric properties characterization

3.2.1. Characteristics of the OLEDs with the plasma-treated ITO

Figs. 7 and 8 show the current–voltage (I–V) and luminance–current density (L–J) characteristics of the fabricated OLEDs with the structure of ITO/TPD/Alq$_3$/Al (without and with O_2 plasma treatment for 5 min, 10 min and 20 min, respectively). In these figures, characteristic curves of the OLEDs with the O_2 plasma treated ITO anode were compared with those of the OLEDs with the as-received ITO anode. On observing Fig. 7, it is clear that hole injection becomes effective if the ITO surface is treated by O_2 plasma; therefore, a decrease of drive voltage follows. This effect is shown even more remarkably by the device with ITO O_2-plasma-treated for 10 min. However, the effect seems to decrease for the device with ITO
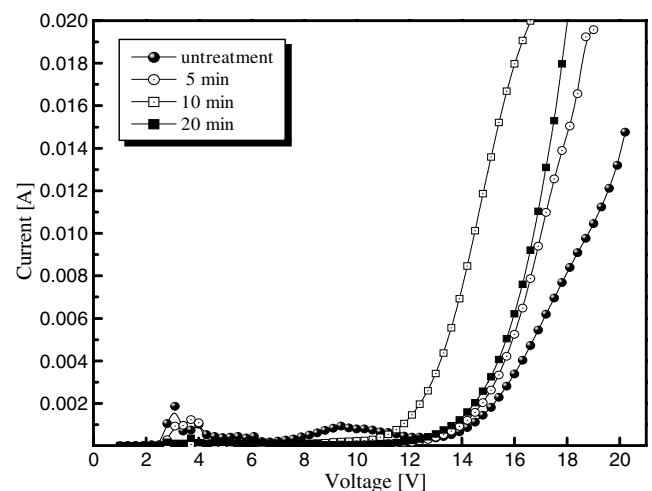

Fig. 7. Current–voltage characteristics of OLEDs without and with O_2 plasma treatment for 5 min, 10 min and 20 min, respectively.
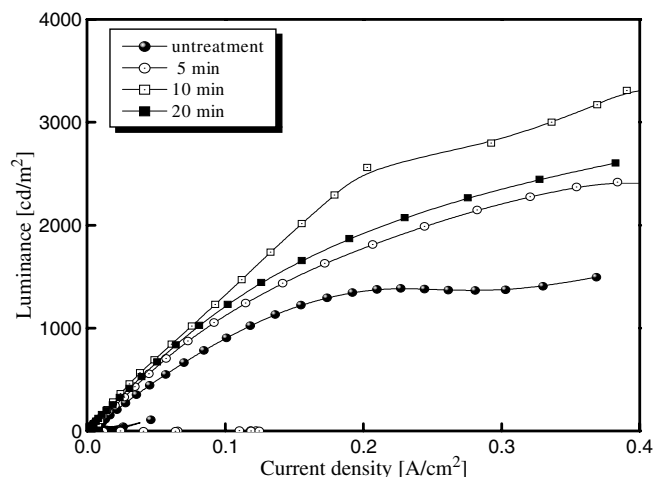
Fig. 8. Luminance–current density characteristics of OLEDs without with and O$_2$ plasma treatment for 5 min, 10 min and 20 min, respectively.
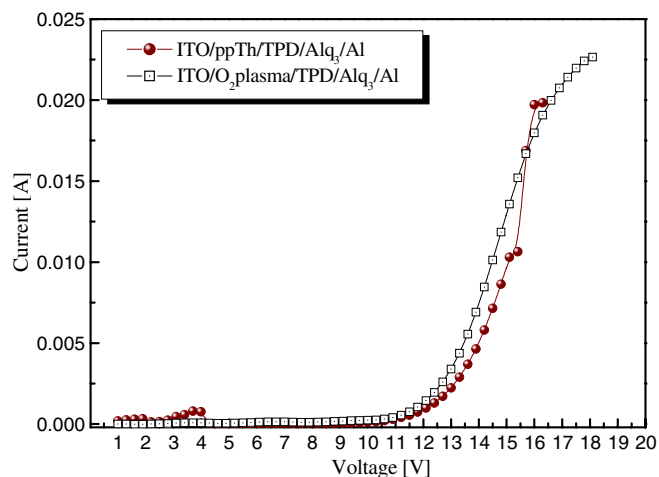

Fig. 9. Current–voltage characteristics of OLEDs as increased due to the introduction of the thin ppTh layer.
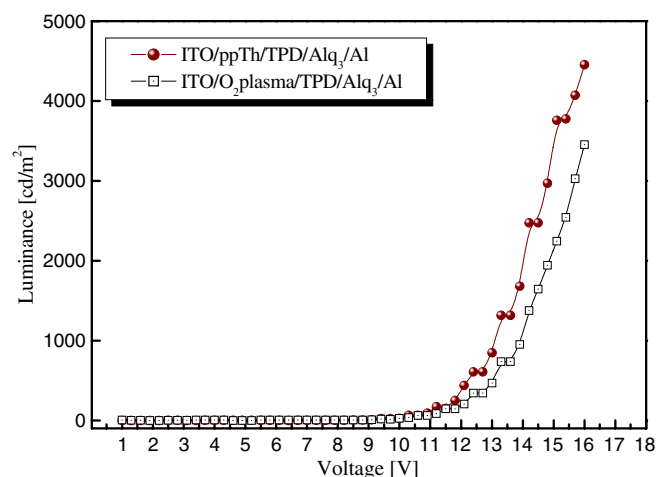

Fig. 10. Luminance–voltage characteristics of OLEDs as increased due to the introduction of the thin ppTh layer.

O$_2$-plasma-treated for 20 min, because degradation of the surface is generated by long time O$_2$ plasma irradiation. Fig. 8 shows that luminance increased after the O$_2$ plasma treatment of the ITO. However, the highest luminance is observed for the device of which the ITO surface was treated by O$_2$ plasma for 10 min, whilst the one with ITO treated for 20 min shows somewhat decreased luminance. Thus, in this work, 10 min is the best time for ITO surface treatment by O$_2$ plasma. It is generally known that work function interface equilibrium, as well as morphology, is an effective factor for the function of OLEDs. When the ITO surface is treated by O$_2$ plasma, the work function becomes 0.5 eV higher than when it is not treated. Therefore hole injection to the light-emitting layer increases [13]. As a result, the drive voltage becomes low and the device proton efficiency increases. The effect of surface morphology can also be suggested. In OLEDs, the interface effect of the organic/ITO thin film is therefore very important.

3.2.2. Characteristics of the OLEDs with ppTh buffer layer

In this work, ppTh was prepared as the buffer layer and the effect of ppTh on the device efficiency was investigated. The device structure is then a in the form of ITO/ppTh/TPD/Alq$_3$/Al. Thickness of the ppTh was 2 nm. The performance of the device with the ppTh buffer layer was compared with that of the device with ITO O$_2$-plasma-treated for 10 min.

Fig. 9 shows current voltage characteristics of the OLEDs. Current of the device with the ppTh buffer layer is lower at the same given voltage. It is considered that the ppTh is an insulating film [11]. Unlike the OLEDs with the CuPc buffer layer [14], the turn-on voltage of the devices with the ppTh buffer was decreased. Fig. 10 shows luminance–voltage characteristics of OLEDs. An impressive brightness higher than 4600 cd/m^2 was measured for the OLEDs with 2 nm thick ppTh, while the device without ppTh revealed a much lower value of 3400 cd/m^2. Simi-

larly, the luminous efficiency of the OLEDs was increased due to the introduction of the thin ppTh layer (Fig. 11). For the device with the ppTh, a maximal luminous efficiency of 1.8 cd/A is achieved. The ppTh layer studied in this work is an insulator film, which seems to be disadvantageous for hole injection at the interface between the ITO anode and the ppTh layer. On the other hand, the thickness of the ppTh buffer is so small that the hole carriers can be injected into the Alq$_3$ layer through tunneling injection. Furthermore, the redundant holes can be blocked off by the ppTh barrier, and a balance combination can be obtained in the devices. If the thickness of the buffer layer increases, then the EL device will not work. It is assumed that the ITO surface will be fully covered by the insulator. Hole injection will be then suppressed with increased buffer layer thickness, which is supported by the lower current density in the device with increased ppTh over 2 nm. In consequence, plasma-polymerized thiophene films at radio frequency are insulating with extremely high resistivity.
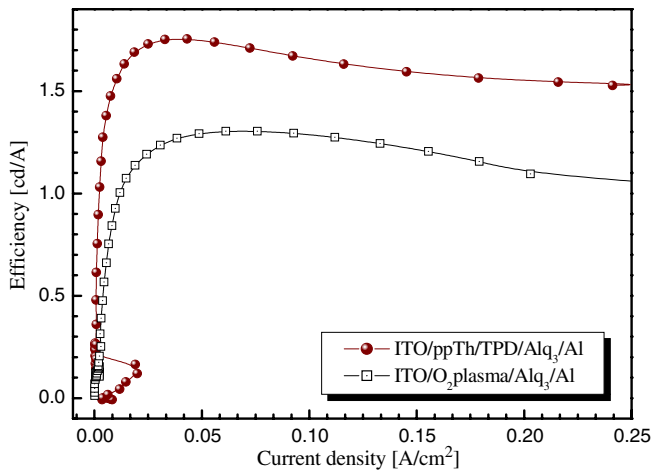
Fig. 11. Efficiency–current density characteristics of the OLEDs as increased due to the introduction of the thin ppTh layer.

Then, the ppTh layer might act as a stable barrier to impede indium diffusion from ITO electrode into TPD layer and thus enhance the device stability.

4. Conclusion

In this research, RF plasma was utilized for anode modification in OLEDs. A possible device performance enhancement of OLEDs was tried by ITO anode surface treatment by using O_2 plasma and inserting a ppTh buffer layer between ITO and HTL. Improved efficiency of the resulting device seemed to be caused by energy changes on the metal/organic interface which might be the kernel in development of OLEDs. The following conclusions were inferred from the study:

(1) The best conditions for plasma surface treatment ware 100 W, 10 sccm, 0.1 torr in oxygen, with treating time of 10 min. Hole injection became effective in the condition of ITO surface treatment with plasma; therefore, drive voltage was reduced and luminance rose.

(2) In the case of the device with an inserted buffer layer fabricated by using the plasma polymerization method, the thickness of the RF plasma polymerized thiophene insulator film was 2 nm. The turn-on voltage of the resulting OLEDs was lower than that of the OLEDs without the buffer layer. In addition, the luminance was improved to 4600 cd/m^2 i.e. higher than that (3400 cd/m^2) of the device without the buffer layer.

References

[1] C.W. Tang, S.A. VanSlyke, Appl. Phys. Lett. 51 (1987) 913.
[2] T. Uchida, T. Mimura, S. Kaneta, M. Ichihara, M. Ohtsuka, T. Otomo, Jap. J. Appl. Phys. 44 (2005) 5939.
[3] J.-H. Lee, N.G. Park, Y.S. Kim, C.-H. Suh, J.-H. Shim, Y.K. Kim, Curr. Appl. Phys. 5 (2005) 9.
[4] H.H. Sung, I.H. Kim, K.N. Byun, H.S. Yoo, Curr. Appl. Phys. 5 (2005).
[5] F.L. Wong, M.K. Fung, S.W. Tong, C.S. Lee, S.T. Lee, Thin Solid Films 466 (2004) 225.
[6] H.T. Lu, M.J. Yokoyama, Cryst Growth 260 (2004) 186.
[7] N.G. Park, M.Y. Kwak, B.O. Kim, O.K. Kwon, Y.K. Kim, B. You, T.W. Kim, Y.S. Kim, Jan. J. Appl. Phys. 41 (2002) 1523.
[8] L.S. Hung, L.R. Zheng, M.G. Mason, Appl. Phys. Lett. 78 (2001) 673.
[9] S.O. Kim, D.C. Lee, J. Korean Phys. Soc. 35 (1999) S708.
[10] K.B. Lim, B.S. Lee, J.T. Kim, D.C. Lee, Surf. Interf. Anal. 33 (2002) 918.
[11] B.S. Lee, D.C. Lee, IEEE Trans. DEI 6 (1997) 907.
[12] M.S. Silverstein, I.V. Fisfe I, Polymer 43 (2002) 11.
[13] M.G. Mason, L.S. Hung, C.W. Tang, S.T. Lee, K.W. Wong, M. Wang, J. Appl. Phys. 86 (1999) 1688.
[14] S.M. Tadayyon, H.M. Grandin, K. Griffths, P.R. Norton, H. Aziz, Z.D. Popovic, Org. Electron. 5 (2004) 157.